IEEE Access
Multidisciplinary | Rapid Review | Open Access Journal

Received 27 January 2023, accepted 12 February 2023, date of publication 22 February 2023, date of current version 8 March 2023.

*Digital Object Identifier 10.1109/ACCESS.2023.3247438*

RESEARCH ARTICLE

# Investigating Performance of BDS-2+3 Dual-Frequency Absolute Positioning With Broadcast Ephemerides, RTS and Final MGEX Products

**SHENGNAN LIU[1,2], SHAOLIN ZHU[2], AND JIAN ZHANG[3]**

[1]School of Civil Engineering, Jiangsu Urban and Rural Construction Vocational College, Changzhou, Jiangsu 213147, China
[2]School of Earth Sciences and Engineering, Hohai University, Nanjing, Jiangsu 211100, China
[3]Powerchina Qinghai Electric Power Design Institute Company Ltd., Xining, Qinghai 210019, China

Corresponding author: Shaolin Zhu (zhushaolin_ch@hhu.edu.cn)

This work was supported in part by the Natural Science General Project of Jiangsu Universities under Grant 21KJB420006; in part by the Changzhou Science and Technology Planning Project under Grant CJ20210053; in part by the "QingLan" Project of Jiangsu Universities (2020, 2022); and in part by the Higher Education Technological Innovation Team Program of Education, Department of Jiangsu Province (2021).

**ABSTRACT** BDS-3 was formally put into service on July 31, 2020, and now along with BDS-2 provides the positioning, navigation and timing services. In this contribution, different techniques of dual-frequency absolute positioning using the fully serviceable BDS-2+3 constellation are evaluated and compared to the positioning performance of GPS constellation. The accuracy of BDS-3 broadcast ephemerides is significantly higher than that of BDS-2 and is comparable to that of GPS, while BDS-3 International GNSS Service (IGS) Real-Time Service (RTS) products are not as good as GPS at this stage. The static Single Point Positioning (SPP) using BDS-2+3 pseudoranges based on broadcast ephemerides attains the positioning accuracy of 0.743/0.601/1.021 m (95%) and 0.453/0.365/0.566 m (68%) in east/north/up components, while its positioning accuracy is 1.210/1.097/2.447 m (95%) and 0.660/0.586/1.264 m (68%) in kinematic mode. BDS-2+3 Precise Point Positioning (PPP) using pseudoranges with carrier-phase observations based on broadcast ephemerides is able to achieve a positioning accuracy of 0.239/0.174/0.529 m (95%) and 0.115/0.096/0.296 m (68%) in static mode, and 0.636/0.486/1.108 m (95%) and 0.304/0.242/0.556 m (68%) in kinematic mode. BDS-2+3 PPP based on final Multi-GNSS Experiment (MGEX) product can obtain the positioning accuracy of centimeter to millimeter in static mode and the centimeter-level positioning accuracy in kinematic mode. The experiment results show that the positioning performances of BDS-2+3 using broadcast ephemerides and final MGEX products are both comparable to those of GPS. However, due to the poor quality and incomeless of BDS IGS RTS product, BDS-2+3 SPP and PPP based on IGS RTS product obtain the poor positioning accuracies in both static and kinematic modes, which are obviously worse than the counterparts of GPS. Another remarkable result can be obtained that BDS-2+3 achieves a better positioning performance in Asia-Pacific region at higher cut-off elevations as compared to GPS positioning.

**INDEX TERMS** BDS-2/BDS-3, precise point positioning (PPP), single point positioning (SPP), broadcast ephemerides, real-time service (RTS), multi-GNSS experiment (MGEX).

## I. INTRODUCTION

As one of the Global Navigation Satellite Systems (GNSSs), Chinese BDS, according to the "three-step" strategy, has been developed from the demonstration system (BDS-1) to the regional system (BDS-2) and finally the global system (BDS-3) [1]. Different from other GNSSs, both BDS-2 and BDS-3 consist of three types of orbiting satellites: Geostationary Earth Orbit (GEO), Inclined Geostationary Orbit (IGSO) and Medium Earth Orbit (MEO) satellites. Since

The associate editor coordinating the review of this manuscript and approving it for publication was Riccardo Carotenuto.

the launch of BDS-2 satellites, many scholars have made thorough and sufficient research on the observation bias, relative positioning, absolute positioning and so on. During the construction of BDS-3 constellation, a series of valuable studies were published, including signal performance analysis [2], [3], satellite precise orbit determination [4], [5] and inter-satellite measurement evaluation [6].

The relative positioning performance of BDS-2 and BDS-3 combined with other GNSSs has been investigated. The performance of BDS precise relative positioning has been evaluated [7], [8] and some methods of tight integration of BDS-3 and other GNSSs are proposed to improve the RTK (real-time kinematic) ambiguity fixing efficiency and positioning accuracy [8], [9], [10]. Compared with the absolute positioning, the relative positioning has the disadvantage of high cost of maintaining base stations or reference network. Single Point Positioning (SPP) adopting pseudorange observations and broadcast ephemerides realizes the first absolute positioning technology, which achieves the positioning accuracy of several meters. It is announced that BDS has a global coverage of horizontal and vertical positioning accuracy of up to 10 meters (95%) and timing accuracy of better than 20 nanoseconds [11]. Many scholars have studied the BDS-2+3 combined SPP, and found that a time delay bias parameter needs to be added to the SPP positioning model [12], [13], [14], [15]. After estimating the time delay bias in positioning model, the SPP performance is able to be improved.

To improve the accuracy of absolute positioning, International GNSS Service (IGS) utilizes the observations from the GNSS stations around the world to start publishing the precise satellite orbit and clock, and this has now been developed to the Multi-GNSS Experiment (MGEX) product [16]. Also, the BDS-2+3 combined PPP has been studied, and it is found that the optimal positioning performance can be obtained when time delay bias is estimated to be constant [15], [17], [18], [19], [20]. The accuracy of SPP is much lower than that of RTK, and PPP technology using precise satellite products from IGS or MGEX provides an alternate technology for RTK. However, PPP based on MGEX products is a post-processing method and does not provide the real-time positioning. Therefore, IGS started the Real-Time Service (RTS) since August 2011. Furthermore, Centre National d'Études Spatiales (CNES) analysis center can support the RTS products for all available GNSS. On the other hand, the absolute positioning using pseudorange and carrier-phase observations based on broadcast ephemerides is able to achieve the positioning accuracy of several decimeters [21], [22]. In conclusion, GNSS PPP can be obtained by using a receiver that can track carrier phase measurements in real-time mode, that is, using a broadcast ephemeris with or without RTS correction, and in post-processing mode, that is, using the final MGEX product.

Most of the researches mainly focused on the absolute positioning of BDS-3 experimental satellites or BDS-3 preliminary system [23], [24]. With the formal completion of

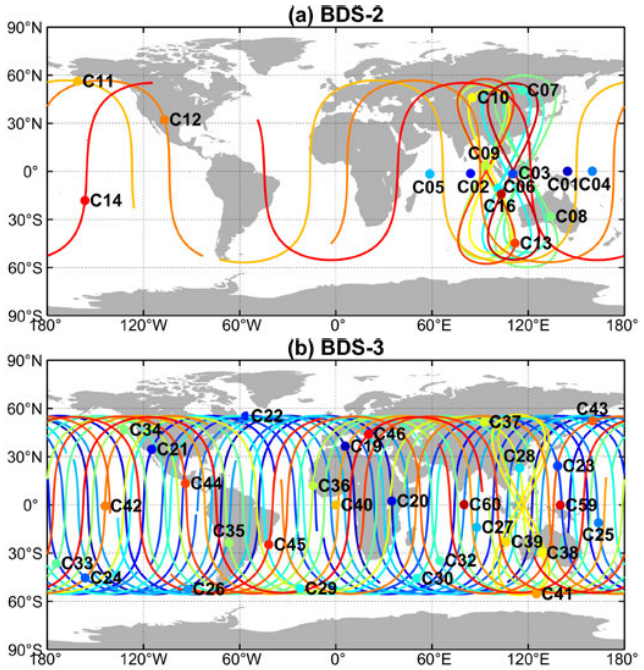


**FIGURE 1.** BDS-2 (top) and BDS-3 (bottom) ground tracks on DOY 228 of 2021 with satellite locations (dots) at BDT 20:00 PM. Each color in the figure refers to a BDS satellite.

BDS-3 global constellation, the availability of a large number of available BDS-2+3 satellites and supporting products finally enables us to use different ephemeris products to perform BDS-2+3 positioning globally in real-time and post-processing mode. In addition, we also fully compare the absolute positioning performance of BDS-2+3 and GPS in a global scale and a specific one i.e., Asia-Pacific region. This work conducts a comprehensive study of BDS-2+3 absolute positioning, which is conducive to the global application of BDS.

This work focuses on the dual-frequency absolute positioning performance of BDS-2+3 based on broadcast ephemerides, RTS and final MGEX products using pseudorange or pseudorange +carrier-phase observations. The satellite availability and PDOP of BDS-2+3 are first introduced and compared with GPS. Following that, the experimental data and processing strategies are described. Then, we assess the orbit and clock quality of broadcast ephemerides and RTS products for BDS-2+3 and GPS. Afterward, the dual-frequency absolute positioning performance of BDS-2+3 is evaluated in static and kinematic modes and compared with GPS positioning solutions. Finally, the summary and conclusions are presented.

## II. SATELLITE AVAILABILITY AND PDOP

Table 1 shows the space segment composition of BDS-2 and BDS-3 as of August 2021. With the exception of C61, all BDS-2 and BDS-3 satellites can be used for positioning and navigation. Figure 1 exhibits the ground tracks of all BDS-2 and BDS-3 satellites. As the main GEO and IGSO

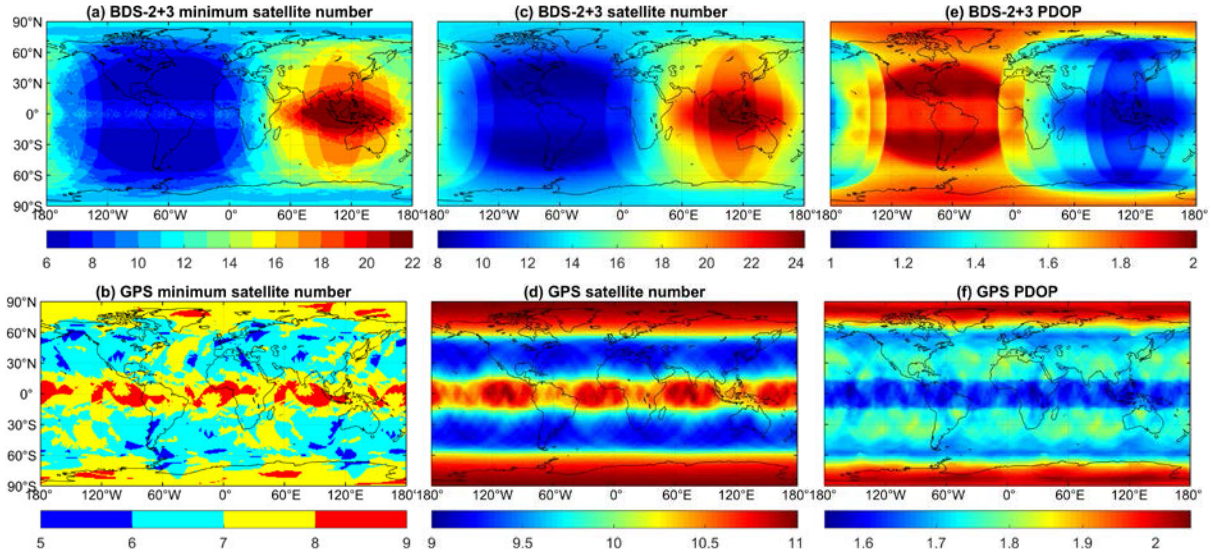


**FIGURE 2.** Minimum (left) and average number (central) of visible satellites and average PDOP (right) for BDS-2+3 (top) and GPS (bottom) with 7° cut-off elevation. The data span is DOY (Day of Year) 228-234 of 2021.

satellites of regional BDS-2 are located in the Asia-Pacific region, it mainly serves the Asia-Pacific region. Different from BDS-2, the global BDS-3 mostly includes MEO satellites which provide the positioning, navigation and timing services worldwide. To make a comparison of satellite visibility and Position Dilution of Precision (PDOP), Figure 2 presents the minimum and average number of visible satellites and average PDOP for BDS-2+3 and GPS in a one-week period. After subdividing the earth surface with a $1°\times1°$ grid at zero altitudes, the minimum and average values of satellite number and PDOP are computed for each cell midpoints based on the observation data on DOY (Day of Year) 228-234 of 2021 and with an elevation mask of 7°. It can be found that the satellite visibility distribution of BDS-2+3 is presented as two large elliptical regions, and the satellite visibility in the eastern hemisphere is better than that of western hemisphere. The reason is that the IGSO and GEO satellites of BDS-2 and BDS-3 mainly serve the eastern hemisphere. For the minimum number of satellites in BDS-2+3, there are at least 6 visible satellites in an elliptical area (60° N-60° S and 0°-150° W), and at least 14 visible satellites can be observed in another elliptical area (60° N-60° S, 40° E-180° E). As for GPS, the minimum satellite number varies from 5 to 9, and the minimum number of satellites is the largest at the equator and two poles. On average, there are 8-12 visible satellites in the west elliptical region, while the corresponding numbers increase to 16-24 for the east elliptical region. In addition, an average of 11 to 15 satellites can be tracked outside the two elliptical regions. In the case of GPS, the number of visible satellites in the 15°-60°N and 15°-60°S latitude regions is only 9-10, while the corresponding number of satellites in other regions is 10-11. Similar to the distribution of visible number of satellites, the distribution of PDOP values of BDS-2+3 also presents two elliptic regions, 1.6-2.0 and 1.0-1.5, respectively. For the regions beyond the two ellipses, the PDOP value of BDS-2+3 is 1.4-1.8. As for GPS, in the areas from 60° S to 60° N, the PDOP value initially decreases from 1.80 to 1.55 and then increases to 1.80 with the increase of latitude, while in the regions above 60°, the corresponding value is 1.85-2.05. It can be concluded that the system availability of BDS-2+3 in the Asia-Pacific region is better than that of GPS, and their satellite availability and PDOP in other regions is basically equivalent.

**TABLE 1.** Space segment of BDS-2 AND BDS-3 as of August 2021.

| System | PRN | Type |
|---|---|---|
| BDS-2 | C01, C02, C03, C04, C05 | GEO (5) |
| | C06, C07, C08, C09, C10, C13, C16 | IGSO (7) |
| | C11, C12, C14 | MEO (3) |
| BDS-3 | C59, C60, C61 (Testing) | GEO (3) |
| | C38, C39, C40 | IGSO (3) |
| | C19, C20, C21, C22, C23, C24, C25, C26, C27, C28, C29, C30, C32, C33, C34, C35, C36, C37, C41, C42, C43, C44, C45, C46 | MEO (24) |

## III. EXPERIMENTAL DATA AND PROCESSING STRATEGIES

### A. EXPERIMENTAL DATA

The BDS-2 and BDS-3 broadcast ephemerides (BRDC) can be obtained through Wuhan University (WHU) analysis center (ftp://igs.gnsswhu.cn/pub/gps/data/). The multi-GNSS (including BDS-2, BDS-3 and GPS) RTS products from CNES analysis center are adopted. The real-time corrections of broadcast orbits and clocks can be obtained from CNES's real-time stream CLK93 (http://www.ppp-wizard.net/products/REAL_TIME/). Its clock offsets are computed with the use of B1I and B3I dual-frequency ionosphere-free (IF) combination. The final Multi-GNSS

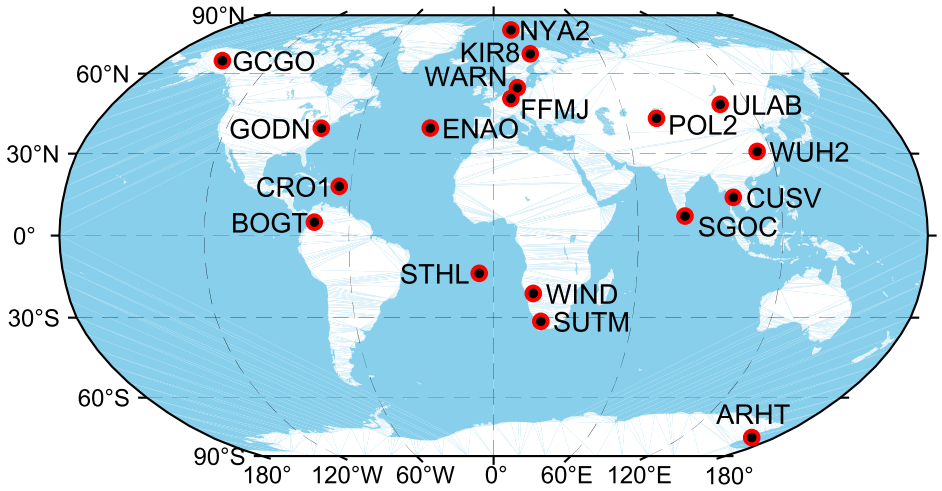


**FIGURE 3.** Geographical distribution of 18 global MGEX stations.

Experiment (MGEX) products are provided by WHU analysis center (ftp://igs.gnsswhu.cn/pub/gps/products/mgex/). It should be mentioned that the broadcast ephemerides provide the orbit and clock of satellites with maximum PRN (Pseudo Random Noise) to C60, the RTS products from CNES analysis center to C37, and the final MGEX products from WHU analysis center to C46. In addition, the 30-day observations on DOY 228-257 of 2021 from 18 global MGEX stations are selected to evaluate the performance of dual-frequency pseudorange and carrier-phase absolute positioning. The sampling interval of observations at these stations is 30s. All these MGEX stations can observe the observations of BDS-2, BDS-3 and GPS and their geographical distribution is exhibited in Figure 3. The missing rate of BDS and GPS RTS products in the selected consecutive period is less than 5% per day, so as to thoroughly analyze the positioning performance of real-time PPP based on RTS products.

### B. PROCESSING STRATEGIES OF DUAL-FREQUENCY ABSOLUTE POSITIONING

The dual-frequency observations are processed using undifferenced and uncombined function model [25]. The undifferenced and uncombined pseudorange and carrier-phase observations from satellite $s$ to receiver $r$ on the i-th frequency can be respectively written as,

$$\begin{aligned} P_{r,i}^{s,Q} &= \rho_r^{s,Q} + cdt_r - cdt^{s,Q} + T_r^{s,Q} + \gamma_i^Q \cdot I_{r,1}^{s,Q} \\ &\quad + d_{r,i}^Q - d_i^{s,Q} + \varepsilon_{r,i}^{s,Q} \end{aligned} \tag{1}$$

$$\begin{aligned} L_{r,i}^{s,Q} &= \rho_r^{s,Q} + cdt_r - cdt^{s,Q} + T_r^{s,Q} - \gamma_i^Q \cdot I_{r,1}^{s,Q} \\ &\quad + N_{r,i}^{s,Q} + b_{r,i}^Q - b_i^{s,Q} + \xi_{r,i}^{s,Q} \end{aligned} \tag{2}$$

where $P_{r,i}^{s,Q}$ and $L_{r,i}^{s,Q}$ are the pseudorange and carrier-phase observations, respectively; superscript Q refers the system, which can be C3 or C2 indicating BDS-3 or BDS-2, respectively; $\rho_r^{s,Q}$ represents the geometric distance between satellite and receiver; $cdt_r$ and $cdt^{s,Q}$ represent the receiver and satellite clock offsets, respectively; $T_r^{s,Q}$ denotes the tropospheric delay; $I_{r,1}^{s,Q}$ denotes the ionospheric delay with the frequency-dependent amplification factor $\gamma_i^Q = f_1^{s,Q}/f_i^{s,Q}$, where $f_i^{s,Q}$ is the $i$-th frequency; $N_{r,i}^{s,Q}$ represents the phase ambiguity in meter; $d_{r,i}^Q$ and $d_i^{s,Q}$ represent the uncalibrated code delays (UCDs) at receiver and satellite; $b_{r,i}^Q$ and $b_i^{s,Q}$ denote the uncalibrated phase delays (UPDs) at receiver and satellite; and $\varepsilon_{r,i}^{s,Q}$ and $\xi_{r,i}^{s,Q}$ represent the measurement noises of pseudorange and carrier-phase observations.

#### 1) BDS-2+3 SPP BASED ON BROADCAST EPHEMERIDES AND RTS PRODUCT

In the BDS-2+3 combined SPP, a parameter, i.e., time delay bias (TDB) between BDS-2 and BDS-3, is necessary to be introduced to the function model [26]. After correcting the satellite orbit and clock and the tropospheric delays, the linearized BDS-2+3 pseudorange-based absolute positioning model can be expressed as,

$$\begin{cases} p_{r,i}^{s,C3} = \mathbf{u}_r^{s,C3} \cdot \mathbf{x} + c\hat{dt}_r + \gamma_i^{C3} \cdot \hat{I}_{r,1}^{s,C3} + \varepsilon_{r,i}^{s,C3} \\ p_{r,i}^{s,C2} = \mathbf{u}_r^{s,C2} \cdot \mathbf{x} + c\hat{dt}_r + \mathrm{TDB} - \gamma_i^{C2} \cdot \hat{I}_{r,1}^{s,C2} + \varepsilon_{r,i}^{s,C2} \end{cases} \tag{3}$$

$$\begin{cases} c\hat{dt}_r = cdt^{s,C3} + d_{r,IF_{12}}^{C3},\ d_{r,IF_{12}}^{C3} = \alpha_{12}^{C3} \cdot d_{r,1}^{C3} - \beta_{12}^{C3} \cdot d_{r,2}^{C3} \\ \hat{I}_{r,1}^{s,Q} = I_{r,1}^{s,Q} + \beta_{12}^Q \cdot \mathrm{DCB}_{r,12}^Q,\ \mathrm{DCB}_{r,12}^Q = d_{r,1}^Q - d_{r,2}^Q \end{cases} \tag{4}$$

where $p_{r,i}^{s,Q}$ denotes the observed-minus-computed (OMC) value of pseudorange observation; $i = 1, 2$ represents B1I and B3I frequency signals, respectively; $u_r^{s,Q}$ is the unit vector of satellite-receiver direction; $\mathbf{x}$ denotes the three-dimensional position increment relative to the initial coordinates; $c\hat{dt}_r$ denotes the re-parameterization of receiver clock offset absorbing the ionosphere-free receiver UCDs; TDB represents the time delay bias between BDS-2 and BDS-3; $\hat{I}_{r,1}^{s,Q}$ denotes the ionospheric delay absorbing the receiver DCB (differential code bias).

The Kalman filter is adopted to resolve the positioning model, and the parameters of each epoch are estimated. The

estimated parameters, including the positions, receiver clock offset, time delay bias and ionospheric delays for n tracked satellites, can be written as,

$$\boldsymbol{X}_{sb} = \left[\Delta x,\, \Delta y,\, \Delta z,\, c\hat{dt}_r,\, \mathrm{TDB},\, \hat{I}_{r,1}^{1,\mathrm{Q}}, \cdots, \hat{I}_{r,1}^{n,\mathrm{Q}}\right]^T \quad (5)$$

### 2) BDS-2+3 PPP BASED ON BROADCAST EPHEMERIDES

The functional model in Eq. (3) only utilizes the pseudorange observations, which will not make full use of the observations observed by the receivers. In the BDS-2+3 combined PPP using pseudorange and carrier-phase observations, a TDB parameter between BDS-2 and BDS-3 also needs to be added to the function model [19]. Finally, the BDS-2+3 PPP function model based on broadcast ephemerides can be written as,

$$\begin{cases} p_{r,i}^{s,\mathrm{C3}} = \mathbf{u}_r^{s,\mathrm{C3}} \cdot \mathbf{x} + c\hat{dt}_r + M_\mathrm{w} \cdot Z_\mathrm{w} + \gamma_i \cdot \hat{I}_{r,1}^{s,\mathrm{C3}} \\ \quad + S_r^{s,\mathrm{C3}} + \varepsilon_{r,i}^{s,\mathrm{C3}} \\ l_{r,i}^{s,\mathrm{C3}} = \mathbf{u}_r^{s,\mathrm{C3}} \cdot \mathbf{x} + c\hat{dt}_r + M_\mathrm{w} \cdot Z_\mathrm{w} - \gamma_i \cdot \hat{I}_{r,1}^{s,\mathrm{C3}} \\ \quad + \hat{N}_{r,i}^{s,\mathrm{C3}} + S_r^{s,\mathrm{C3}} + \xi_{r,i}^{s,\mathrm{C3}} \\ p_{r,i}^{s,\mathrm{C2}} = \mathbf{u}_r^{s,\mathrm{C2}} \cdot \mathbf{x} + c\hat{dt}_r + \mathrm{TDB} + M_\mathrm{w} \cdot Z_\mathrm{w} \\ \quad + \gamma_i \cdot \hat{I}_{r,1}^{s,\mathrm{C2}} + S_r^{s,\mathrm{C2}} + \varepsilon_{r,i}^{s,\mathrm{C2}} \\ l_{r,i}^{s,\mathrm{C2}} = \mathbf{u}_r^{s,\mathrm{C2}} \cdot \mathbf{x} + c\hat{dt}_r + \mathrm{TDB} + M_\mathrm{w} \cdot Z_\mathrm{w} \\ \quad - \gamma_i \cdot \hat{I}_{r,1}^{s,\mathrm{C2}} + \hat{N}_{r,i}^{s,\mathrm{C2}} + S_r^{s,\mathrm{C2}} + \xi_{r,i}^{s,\mathrm{C2}} \end{cases} \quad (6)$$

where $l_{r,i}^{s,Q}$ denotes the carrier-phase OMC value; $S_r^{s,Q}$ represents the SISRE value for each tracked satellite; $Z_\mathrm{w}$ is the tropospheric zenith wet delay and $M_\mathrm{w}$ is the corresponding wet mapping function; $\hat{N}_{r,i}^{s,Q}$ represents the carrier-phase ambiguity assimilating the UCDs and UPDs at receiver and satellite. It should be noted that due to the accuracy limitation of broadcast ephemerides, the BDS-2+3 PPP based on broadcast ephemerides adopts the SISRE parameter to compensate the observations. The estimated parameters can be summarized as,

$$\begin{aligned} \boldsymbol{X}_{pb} = [&\Delta x,\, \Delta y,\, \Delta z,\, c\hat{dt}_r,\, \mathrm{TDB},\, \hat{I}_{r,1}^{1,\mathrm{Q}}, \cdots, \hat{I}_{r,1}^{n,\mathrm{Q}}, \\ &\hat{N}_{r,i}^{1,\mathrm{Q}}, \cdots, \hat{N}_{r,i}^{n,\mathrm{Q}}, S_r^{1,\mathrm{Q}}, \cdots S_r^{n,\mathrm{Q}}]^\mathrm{T} \end{aligned} \quad (7)$$

### 3) BDS-2+3 PPP BASED ON RTS AND MGEX PRODUCTS

The functional model in Eq. (3) achieves the low-precision positioning with an accuracy of 2-3 orders of magnitude lower than PPP using carrier-phase observations. After applying the satellite orbit and clock to observations, the BDS-2+3 combined PPP function model based on MGEX or RTS products using pseudorange with carrier-phase observations can be written as,

$$\begin{cases} p_{r,i}^{s,\mathrm{C3}} = \mathbf{u}_r^{s,\mathrm{C3}} \cdot \mathbf{x} + c\hat{dt}_r + M_\mathrm{w} \cdot Z_\mathrm{w} + \gamma_i \cdot \hat{I}_{r,1}^{s,\mathrm{C3}} + \varepsilon_{r,i}^{s,\mathrm{C3}} \\ l_{r,i}^{s,\mathrm{C3}} = \mathbf{u}_r^{s,\mathrm{C3}} \cdot \mathbf{x} + c\hat{dt}_r + M_\mathrm{w} \cdot Z_\mathrm{w} - \gamma_i \cdot \hat{I}_{r,1}^{s,\mathrm{C3}} + \hat{N}_{r,i}^{s,\mathrm{C3}} \\ \quad + \xi_{r,i}^{s,\mathrm{C3}} \\ p_{r,i}^{s,\mathrm{C2}} = \mathbf{u}_r^{s,\mathrm{C2}} \cdot \mathbf{x} + c\hat{dt}_r + \mathrm{TDB} + M_\mathrm{w} \cdot Z_\mathrm{w} \\ \quad + \gamma_i \cdot \hat{I}_{r,1}^{s,\mathrm{C2}} + \varepsilon_{r,i}^{s,\mathrm{C2}} \\ l_{r,i}^{s,\mathrm{C2}} = \mathbf{u}_r^{s,\mathrm{C2}} \cdot \mathbf{x} + c\hat{dt}_r + \mathrm{TDB} + M_\mathrm{w} \cdot Z_\mathrm{w} \\ \quad - \gamma_i \cdot \hat{I}_{r,1}^{s,\mathrm{C2}} + \hat{N}_{r,i}^{s,\mathrm{C2}} + \xi_{r,i}^{s,\mathrm{C2}} \end{cases} \quad (8)$$

The estimated parameters containing the positions, receiver clock offset, time delay bias, ionospheric delays and carrier-phase ambiguity are same to PPP based on broadcast ephemerides, which can be summarized as,

$$\begin{aligned} \boldsymbol{X}_{pp} = [&\Delta x,\, \Delta y,\, \Delta z,\, c\hat{dt}_r,\, TDB,\, \hat{I}_{r,1}^{1,Q}, \cdots, \hat{I}_{r,1}^{n,Q}, \\ &\hat{N}_{r,i}^{1,Q}, \cdots, \hat{N}_{r,i}^{n,Q}]^\mathrm{T} \end{aligned} \quad (9)$$

From the equations (3), (5) and (7), ten positioning models can be obtained, as shown in Table 2. Explain why these ten positioning models are used: (1) The traditional pseudorange-based SPP using broadcast ephemerides and PPP with pseudorange and carrier-phase observations using RTS or final MGEX products are evaluated; (2) RTS products are obtained through providing real-time satellite orbit and clock corrections to broadcast ephemerides, so the performance of SPP using broadcast ephemerides with RTS corrections is also explored; (3) In conventional SPP, the carrier-phase observations are generally discarded, and thus, to make full use of the observations, this work explore how the positioning accuracy of BRDC ephemerides can be achieved based on the pseudorange and carrier-phase observations; (4) To fully evaluate the positioning performance, the kinematic and static modes are both used for positioning. Therefore, these ten positioning models are used to comprehensively investigate the absolute positioning performance of BDS-2+3 and their detailed processing strategies can be seen from Table 2. In addition, in order to compare BDS-2+3 with GPS, this study conducted all ten positioning models for GPS L1+L2 observations.

## IV. ORBIT AND CLOCK QUALITY ANALYSIS FOR BROADCAST EPHEMERIDES AND RTS PRODUCT

We first evaluate the quality of broadcast ephemerides and RTS product using signal-in-space ranging error (SISRE) method. The precise satellite orbit and clock from the final MGEX products exhibit the highest accuracy and thus are treated as the reference [30], [31]. The broadcast ephemerides and RTS product are compared with the reference to derived the orbit errors in the radial ($\Delta r_R$), along-track ($\Delta r_A$) and cross-track ($\Delta r_C$) directions and the clock errors ($\Delta cdt$). The orbit-only contribution to SISRE can be described as [27],

$$\mathrm{SISRE(orb)} = \sqrt{w_R^2 \cdot R^2 + w_{A,C}^2 \cdot (A^2 + C^2)} \quad (10)$$

where $R$, $A$ and $C$ denote the root mean square (RMS) of orbit errors in the radial, along-track and cross-track (RAC) directions, respectively; $w_R^2$ and $w_{A,C}^2$ are the weight factors for the global SISRE associated with a specific constellation. The BDS and GPS weight factors are shown in Table 3 [27]. Analogous to Eq. (5), the combined orbit and clock SISRE is obtained as,

$$\mathrm{SISRE} = \sqrt{[\mathrm{RMS}(w_R \cdot \Delta r_R - \Delta cdt)]^2 + w_{A,C}^2 \cdot (A^2 + C^2)} \quad (11)$$

Considering that broadcast orbits and clocks both refer to APC (antenna phase center) and precise orbits and clocks

**TABLE 2.** Processing strategies of ten absolute positioning models.

| Positioning models | Coordinates | Observations | Satellite orbits and clocks | Satellite biases | Tropospheric delays |
|---|---|---|---|---|---|
| SPPs+BRDC | static | pseudorange | BRDC | 0 | Saastamoinen+GPT |
| SPPs+RTS | - | - | RTS | - | - |
| PPPs+BRDC | - | pseudorange+phase | BRDC | corrected | estimated |
| PPPs+RTS | - | - | RTS | - | - |
| PPPs+MGEX | - | - | MGEX | - | - |
| SPPk+BRDC | kinematic | pseudorange | BRDC | 0 | Saastamoinen+GPT |
| SPPk+RTS | - | - | RTS | - | - |
| PPPk+BRDC | - | pseudorange+phase | BRDC | corrected | estimated |
| PPPk+RTS | - | - | RTS | - | - |
| PPPk+MGEX | - | - | MGEX | - | - |

**TABLE 3.** Values of weight factors $w_R$ and $w^2_{A,C}$ for BDS and GPS.

| Weight factors | BDS (GEO, IGSO) | BDS (MEO) | GPS |
|---|---|---|---|
| $w_R$ | 0.99 | 0.98 | 0.98 |
| $w^2_{A,C}$ | 1/126 | 1/54 | 1/49 |

refer to center of mass (CoM) and APC, respectively, we should use phase center offset (PCO) and phase center variation (PCV) corrections to transfer the broadcast orbits in APC to that in CoM (center of mass). For the case of real-time products, satellite PCO and PCV corrections were not applied because CNES products are referred to satellite APC. In order to get the SISRE(orb), the orbit errors based on earth centered earth fixed (ECEF) need to be converted into the orbit errors based on RAC. Furthermore, the clock offsets of broadcast and precise ephemerides refer to different signals, and this should use time group delay (TGD) corrections to transfer the broadcast clock offsets to the same datum of precise clock offsets. The details of SISRE(orb) and SISRE calculations can be seen from Figure 4.

### A. ACCURACY ANALYSIS OF BROADCAST EPHEMERIDES

The orbit and clock errors of BDS-2 and BDS-3 satellites can be obtained by comparing the broadcast ephemerides with the final MGEX products. Figure 5 displays the orbit errors in three directions and clock errors of all BDS-2 and BDS-3 satellites in the 30-day period. It can be found that the orbit errors of BDS-3 are significantly smaller than those of BDS-2, which is mostly attributed to the BDS-3 inter-satellite links for satellite orbit determination [28]. Moreover, the clock quality of BDS-3 is significantly improved over that of BDS-2, which benefits from the high-precision atomic clocks equipped in satellite [29]. It is easily observed that the orbit accuracy of BDS-2 GEO satellite broadcast ephemerides is obviously poor, which is due to the quasi-stationary characteristic. Due to the high correlation between the orbit parameters and the ambiguity parameters, the observation geometry of GEO satellite is close to static, and the orbit determination error is large [31]. For a comparison, Figure 6 gives the errors of broadcast ephemerides of GPS satellites, and Table 4 makes an accuracy statistic of orbit and clock for BDS-2, BDS-3 and GPS broadcast ephemerides. The orbit accuracy in RAC directions, clock accuracy, SISRE (orb) and SISRE are all given. The orbit accuracies of BDS-3 in RAC directions and SISRE (orb) are 0.17, 0.38, 0.39 and 0.18 m, which are better than those of GPS. The BDS-3 clock accuracy of 0.79 m is slightly worse than that of GPS. The BDS-3 combined orbit and clock SISRE is 0.75, which is comparable to GPS. On the whole, the quality of broadcast ephemerides of BDS-3 is greatly improved as compare to BDS-2 and is at the same level as GPS.

### B. ACCURACY ANALYSIS OF RTS PRODUCT

In addition, the quality evaluation of satellite orbit and clock from RTS product is conducted as well. Figure 7 shows the orbit and clock errors of RTS product for BDS-2 and BDS-3 satellites in the 30-day period and Figure 8 gives the orbit and clock errors of RTS product for GPS satellites, correspondingly. We can find that the orbit and clock errors of BDS-3 are smaller than that of BDS-2, while its quality of RTS product is worse than that of GPS. Affected by the quasi-stationary characteristic of GEO satellites, the quality of BDS-2 GEO satellite orbit of RTS product is obviously poor. Table 5 exhibits the statistical results of orbit and clock accuracies for BDS-2, BDS-3 and GPS RTS products. The BDS-3 orbit accuracies in RAC directions and clock are 0.09, 0.21, 0.11 and 0.28 m, which is better than that of BDS-2 but worse than that of GPS. The SISRE (orb) and SISRE of BDS-3 are 0.09 and 0.25 m, respectively. In summary, the quality of RTS product of BDS-3 is inferior to that of GPS due to the short operating time of BDS-3 constellation and the few BDS-3 monitoring stations. Besides, the accuracy of RTS ephemerides is obviously better than that of broadcast ephemerides.

## V. PERFORMANCE EVALUATION OF BDS-2+3 DUAL-FREQUENCY ABSOLUTE POSITIONING

The positioning performance of BDS-2+3 dual-frequency absolute positioning is assessed using ten positioning models in Table 2. The positioning solutions with static and kinematic modes are both analyzed. Furthermore, the BDS-2+3 dual-frequency absolute positioning is compared with GPS case.

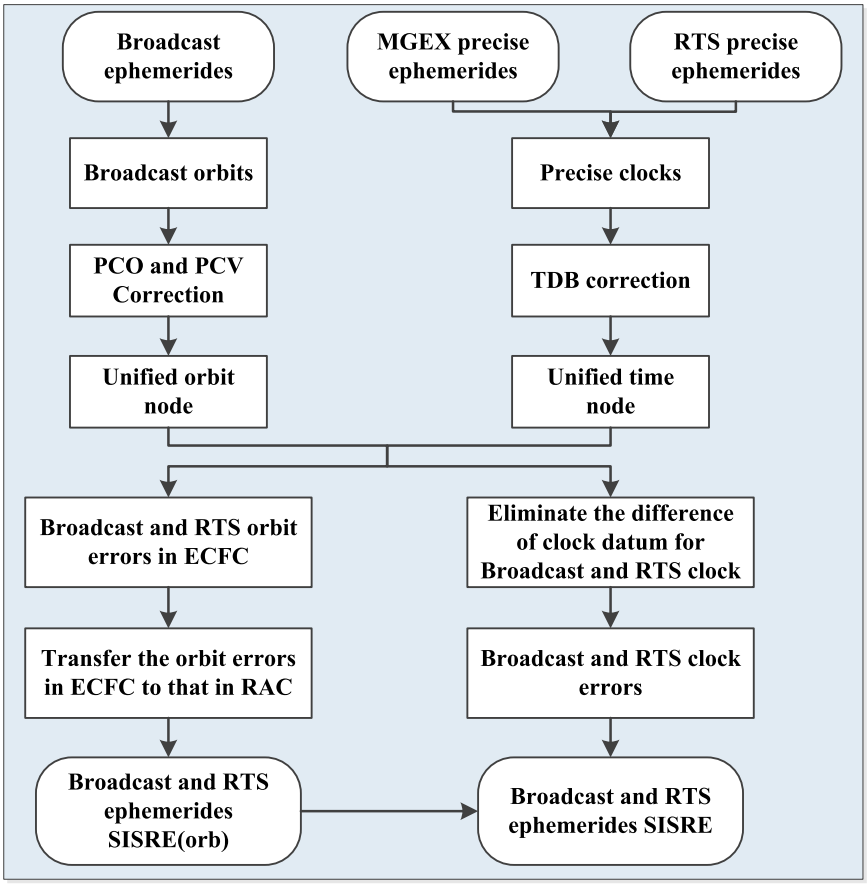


**FIGURE 4.** Flow chart of SISRE (orb) and SISRE calculations for broadcast ephemerides and RTS precise ephemerides.

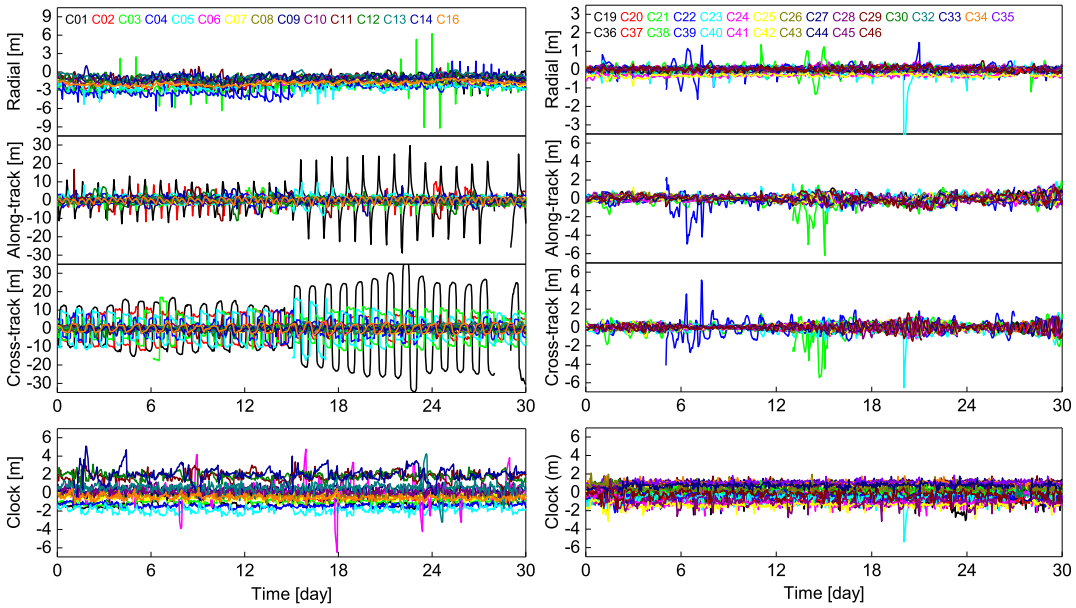


**FIGURE 5.** Orbit and clock errors of broadcast ephemerides compared to MGEX product on DOY 228-257 of 2021 for BDS-2 (left panel) and BDS-3 (right panel) satellites.

### *A. STATIC POSITIONING RESULTS*

Firstly, the BDS-2+3 dual-frequency absolute positioning is conducted with static mode which includes SPPs+BRDC, SPPs+RTS, PPPs+BRDC, PPPs+RTS and PPPs+MGEX. The IGS weekly combined solution was used as the reference value of the station. Figure 9 depicts the time series of

**TABLE 4.** Accuracy statistics of orbit and clock for BDS-2, BDS-3 AND GPS broadcast ephemerides based on mgex product (unit:m).

| Type | Radial | Along-track | Cross-track | Clock | SISRE(orb) | SISRE |
|---|---|---|---|---|---|---|
| **BDS-2** | **1.84** | **2.63** | **6.21** | **1.22** | **1.92** | **1.98** |
| GEO | 2.54 | 4.03 | 10.60 | 1.29 | 2.71 | 1.87 |
| IGSO | 1.47 | 1.08 | 1.68 | 0.62 | 1.47 | 1.52 |
| MEO | 1.10 | 2.30 | 1.31 | 1.95 | 1.14 | 2.92 |
| **BDS-3** | **0.17** | **0.38** | **0.39** | **0.79** | **0.18** | **0.75** |
| IGSO | 0.34 | 0.67 | 0.77 | 0.63 | 0.35 | 0.54 |
| MEO | 0.14 | 0.33 | 0.32 | 0.81 | 0.15 | 0.77 |
| **GPS** | **0.66** | **1.11** | **0.64** | **0.68** | **0.67** | **0.73** |

**TABLE 5.** Accuracy statistics of orbit and clock for BDS-2, BDS-3 and GPS RTS products based on mgex product (unit:m).

| Type | Radial | Along-track | Cross-track | Clock | SISRE(orb) | SISRE |
|---|---|---|---|---|---|---|
| **BDS-2** | **0.30** | **0.95** | **1.83** | **0.33** | **0.35** | **0.35** |
| GEO | 0.50 | 1.66 | 3.23 | 0.49 | 0.59 | 0.55 |
| IGSO | 0.14 | 0.18 | 0.19 | 0.19 | 0.14 | 0.12 |
| MEO | 0.04 | 0.19 | 0.16 | 0.28 | 0.05 | 0.29 |
| **BDS-3 (MEO)** | **0.09** | **0.21** | **0.11** | **0.28** | **0.09** | **0.25** |
| **GPS** | **0.04** | **0.09** | **0.04** | **0.13** | **0.04** | **0.13** |

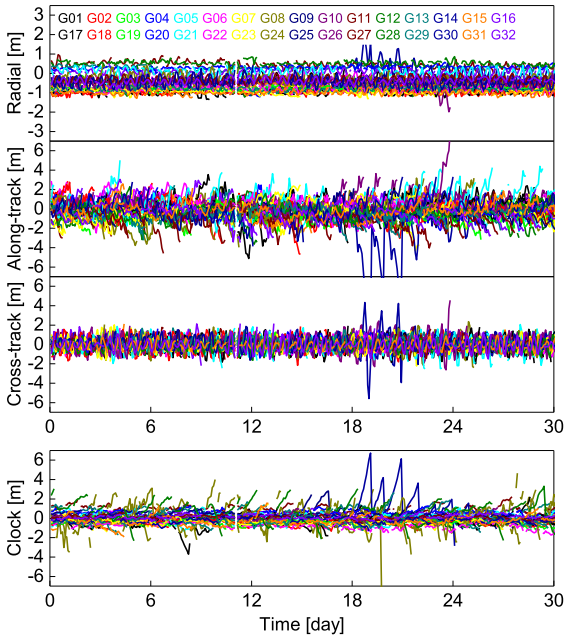


**FIGURE 6.** Orbit and clock errors of broadcast ephemerides compared to MGEX product on DOY 228-257 of 2021 for GPS satellites.

positioning errors obtained from BDS-2+3 static positioning solutions in a one-day period for stations GCGO and ULAB. The positioning errors in the three components are displayed with different color lines indicating different positioning models. It can be found that the positioning errors of SPPs+RTS with high-precision RTS ephemerides are smaller than those of SPPs+BRDC. Furthermore, PPPs+BRDC with pseudorange and carrier-phase observations shows a better positioning accuracy than SPPs+BRDC and SPPs+RTS in three components. Due to the obviously higher accuracy of RTS ephemerides, the positioning accuracy of PPPs+RTS is able to be furthermore improved compared to PPPs+BRDC. Predictably, PPPs+MGEX using final MGEX ephemerides with the highest accuracy has the best positioning accuracy among the five static positioning models. And we can find that the positioning accuracy and convergence performance of PPPs+RTS and PPPs+MGEX are greatly better than those of SPPs+BRDC, SPPs+RTS and PPPs+BRDC.

Subsequently, the statistical results of five positioning models in static mode are calculated to evaluate the positioning performance as a whole. The percentiles in 95%, 68%, 50%, 32% and 5% of absolute positioning errors are accounted for all positioning models. The first 240 epochs are removed to exclude the convergence phase of the Kalman filter and the positioning solutions that show significant deviations from the main distribution are removed from the statistics. After removing the outliers, the statistical results of SPPs+BRDC, SPPs+RTS and PPPs+BRDC positioning models are presented in Fig. 10. It can be found that, the positioning accuracy of SPPs+RTS is better than that of SPPs+BRDC in almost all stations, especially in up component. The higher positioning accuracy is benefited from the RTS real-time ephemerides with high precision and high-frequency ephemeris updates. Although the accuracy of RTS ephemerides is obviously better than that of BRDC ephemerides, the improvement of positioning accuracy of SPPs+RTS compared to SPPs+BRDC is limited. This is because that the positioning performance of SPP mainly depends on the accuracy of pseudorange observation, but its accuracy is in the decimeter level. Using pseudorange and carrier-phase observations based on BRDC ephemerides, PPPs+BRDC model can further improve the positioning accuracy of almost all stations compared with SPPs+BRDC and SPPs+RTS models.

Figure 10 also gives the average positioning accuracy of 18 stations to illustrate the positioning performance of

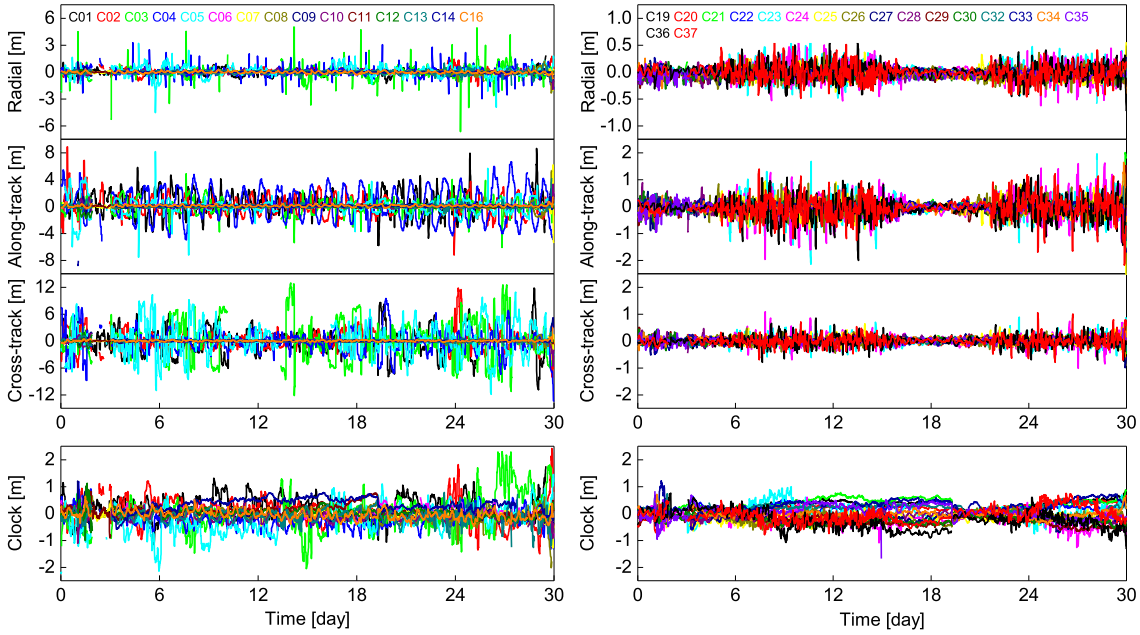


**FIGURE 7.** Orbit and clock errors of RTS product compared to MGEX product on DOY 228-257 of 2021 for BDS-2 (left panel) and BDS-3 (right panel) satellites.

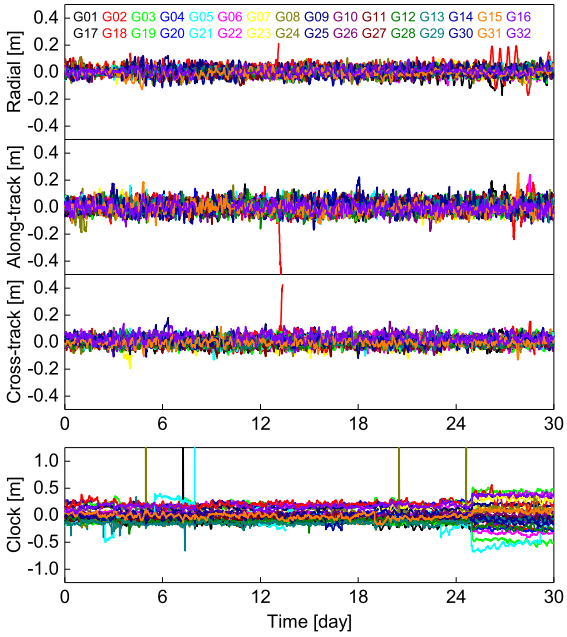


**FIGURE 8.** Orbit and clock errors of RTS product compared to MGEX product on DOY 228-257 of 2021 for GPS satellites.

SPPs+BRDC, SPPs+RTS and PPPs+BRDC models on the whole. Firstly, it is obvious that the positioning accuracy of north component is the highest and that of up component is the lowest. SPPs+RTS model is able to achieve an average positioning accuracy of 0.509/0.404/0.615 m (95%) and 0.353/0.274/0.338 m (68%) in east/north/up components, which is higher than that of 0.743/0.601/1.021 m (95%) and 0.453/0.365/0.566 m (68%) for SPPs+BRDC model. PPPs+BRDC model can achieves a better positioning accuracy of 0.239/0.174/0.529 m (95%) and 0.115/0.096/0.296 m (68%) in east/north/up components. When comparing to SPPs+BRDC model, SPPs+RTS model with high-precision RTS ephemerides only achieves a little higher positioning accuracy, but the PPPs+BRDC with pseudorange and carrier-phase shows a obviously higher positioning accuracy. This means that the positioning accuracy of SPP only using decimeter-accuracy pseudorange observations cannot be greatly improved even using high-precision ephemerides, but the PPP with pseudorange and carrier-phase observations is able to obtain a good positioning accuracy even using low-precision BRDC ephemerides.

Similarly, Figure 11 exhibits the 30-day statistic of PPPs+RTS and PPPs+MGEX positioning solutions for 18 MGEX stations, and the average 95% and 68% positioning accuracy of all positioning solutions are also shown in figure. It is clear that the positioning accuracy of PPPs+MGEX model is obviously higher than that of PPPs+RTS. This is because that the quality of real-time RTS products is inferior to that of final MGEX products. Another obvious phenomenon is that the positioning accuracy of PPPs+RTS and PPPs+MGEX model is more than one order of magnitude higher than that of PPPs+BRDC, although they all use pseudorange and carrier-phase observations. This indicates that when utilizing the carrier-phase observations with millimeter accuracy, the positioning performance is dominated by the accuracy of satellite ephemerides. PPPs+RTS model is able to achieve the average positioning accuracy of

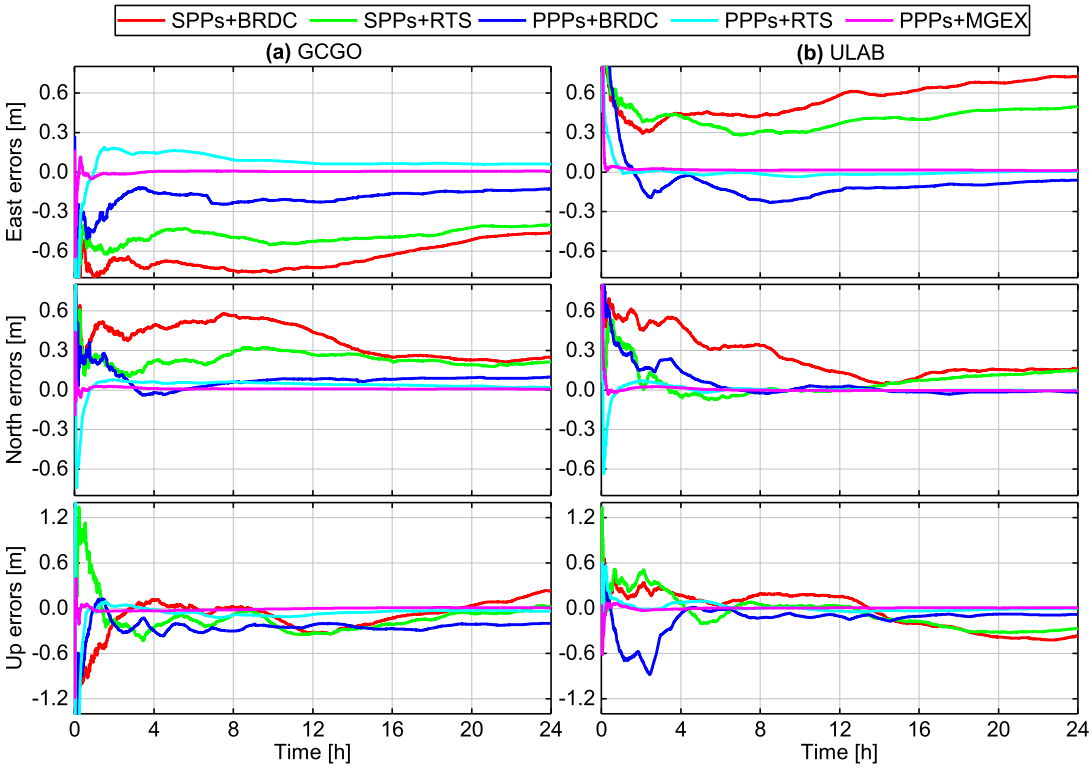


**FIGURE 9.** Daily time series of positioning errors for BDS-2+3 static solutions at stations GCGO and ULAB on DOY 228 of 2021.

0.042/0.026/0.067 m (95%) and 0.018/0.012/0.034 m (68%) in east/north/up components, which is worse than that of 0.014/0.013/0.028 m (95%) and 0.007/0.007/0.015 m (68%) for PPPs+MGEX model.

### B. KINEMATIC POSITIONING RESULTS

The BDS-2+3 dual-frequency absolute positioning is also conducted for five kinematic positioning models. The positioning errors in the three components of stations GCGO and ULAB for five kinematic positioning models are displayed in Figure 12. It can be seen that, the positioning errors of PPPk+BRDC model are smaller and smoother than those of SPPk+BRDC and SPPk+RTS models. Furthermore, the positioning errors of PPPk+RTS model are significantly smaller than those of PPPk+BRDC model. Nevertheless, the positioning errors of PPPk+RTS model show some fluctuations near the zero value as compared to PPPk+MGEX model.

For analyzing the 30-day statistics of positioning accuracy, Figure 13 exhibits the probability distributions of positioning errors in the three components for SPPk+BRDC, SPPk+RTS and PPPk+BRDC models. The 95% and 68% percentiles of absolute positioning errors are also given in figure. Firstly, the average values of positioning errors of three positioning models are at decimeter level for the three components. Secondly, the positioning accuracy of SPPk+RTS model is slightly better than that of SPPk+BRDC model. SPPk+RTS model achieves the positioning accuracy of 0.988/0.973/2.072 m (95%) and 0.534/0.500/1.015 m (68%) in east/north/up components, and the positioning accuracy is 1.210/1.097/2.447 m (95%) and 0.660/0.586/1.264 m (68%) for SPPk+BRDC model. Finally, PPPk+BRDC model with pseudorange and carrier-phase observations obtains the best positioning accuracy compared to SPPk+BRDC and SPPk+RTS, which is 0.636/0.486/1.108 m (95%) and 0.304/0.242/0.556 m (68%) in east/north/up components. And it can be found that the accuracy of kinematic positioning mode is worse than that of static positioning mode. As can be seen from Section IV, the accuracy of RTS ephemerides is obviously better than that of BRDC ephemerides. However, limited by the low accuracy of pseudorange observations, the positioning performance of SPPk+RTS is slightly better than that of SPPk+BRDC. On the other hand, PPPk+BRDC using high-precision carrier-phase observations can significantly improve the positioning performance when compared to SPPk+BRDC.

Similarly, Figure 14 exhibits the probability distributions of positioning errors in the three components for PPPk+RTS and PPPk+MGEX models, and the 95% and 68% percentiles of absolute positioning errors are also given as the positioning accuracy. Comparing the positioning accuracy of these two models, PPPk+MGEX with higher-precision MGEX ephemerides shows an obviously better positioning accuracy than PPPk+RTS with real-time RTS

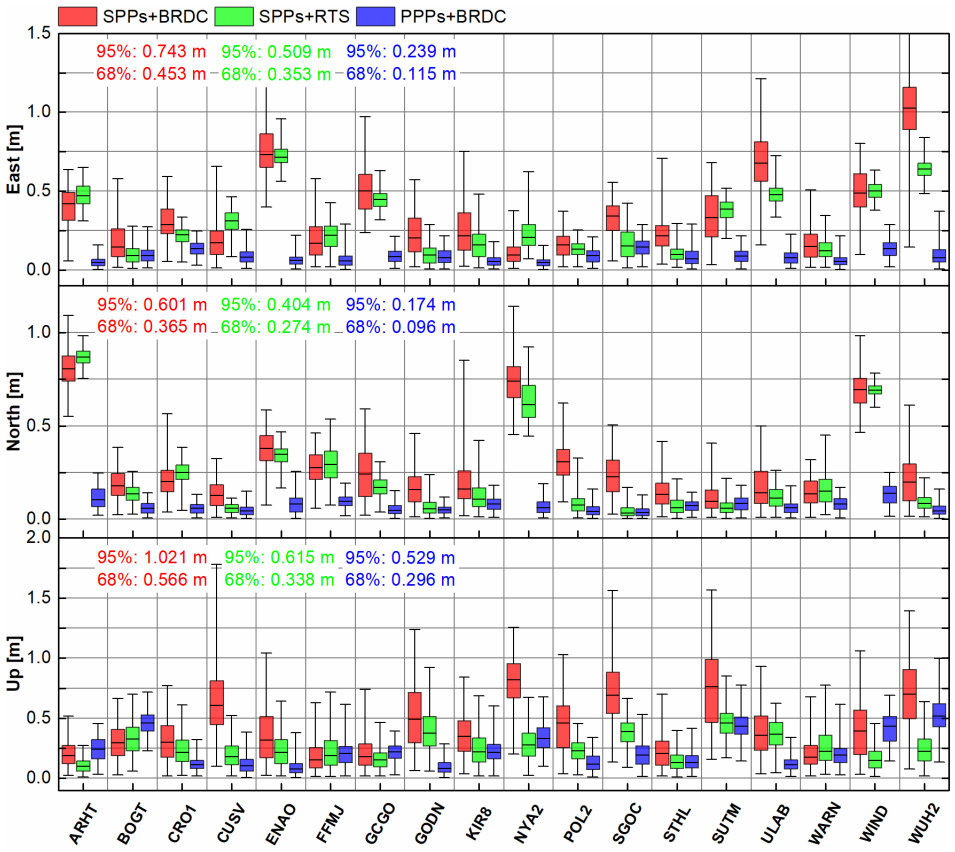


**FIGURE 10.** Distributions of positioning accuracy in the three components on a one-month period for SPPs+BRDC, SPPs+RTS and PPPs+BRDC models. The five short horizontal lines from top to bottom in each box respectively correspond to the 95%, 68%, 50%, 32% and 5% quantiles of absolute positioning errors.

ephemerides. The positioning accuracy of PPPk+MGEX is 0.055/0.037/0.096 m (95%) and 0.022/0.016/0.042 m (68%) in east/north/up components, while the positioning accuracy of PPPk+RTS is 0.142/0.093/0.208 m (95%) and 0.055/0.038/0.091 m (68%). And it is obvious that the positioning accuracy of PPPk+RTS and PPPk+MGEX is more than one order of magnitude higher than that of SPPk+BRDC, SPPk+RTS and PPPk+BRDC.

### C. POSITIONING PERFORMANCE COMPARISON OF BDS-2+3 AND GPS

In this section, the positioning performance of BDS-2+3 is compared with GPS in a global scale with customary cut-off elevation and in the Asia-Pacific region with higher than customary cut-off elevations to investigate the positioning advantages of BDS-2+3 constellation.

#### 1) GLOBAL POSITIONING RESULTS AT CUSTOMARY CUT-OFF ELEVATION

This subsection first compares the positioning performance of BDS-2+3 and GPS with a customary cut-off elevation of 7° in a global scale. The 30-day observations of 18 global MGEX stations in Fig. 3 are processed with ten positioning models for both BDS-2+3 and GPS. The 95% and 68% percentiles of absolute positioning errors are used to evaluate the accuracy of positioning solutions. Table 6 presents the accuracy statistics of BDS-2+3 and GPS dual-frequency static positioning solutions, and Table 7 gives the corresponding results of kinematic positioning solutions in east, north, up and three-dimensional (3D) components. It can be found that for SPP with BRDC ephemerides and PPP with BRDC ephemerides, the positioning accuracy of BDS-2+3 is comparable to that of GPS. However, the positioning accuracy of BDS-2+3 using RTS products is inferior to that of GPS both for SPP and PPP. This is because the accuracy of BDS-2+3 RTS products is not as good as that of GPS RTS products, which can be clearly seen from Table 5. Another reason is that RTS products only provide the BDS-3 orbit and clock with maximum PRN of C37. Fortunately, the positioning performance of BDS-2+3 shows a competitive performance when compared with GPS for PPPs+MGEX and PPPk+MGEX models, which is due to BDS and GPS precise products with commensurate accuracy. With the increasing of tracking stations and more focusing on BDS-3, BDS positioning performance is expected to be further improved in the future with more accurate BDS precise products of orbit, clock and PCO/PCV corrections.

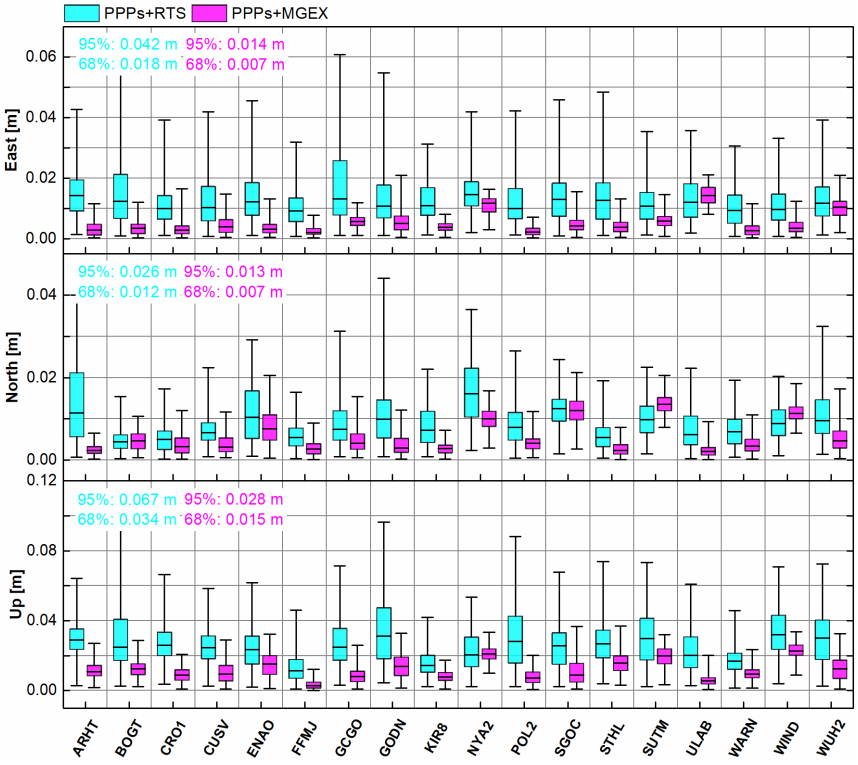


**FIGURE 11.** Distributions of positioning accuracy in the three components on a one-month period for PPPs+RTS and PPPs+MGEX models.

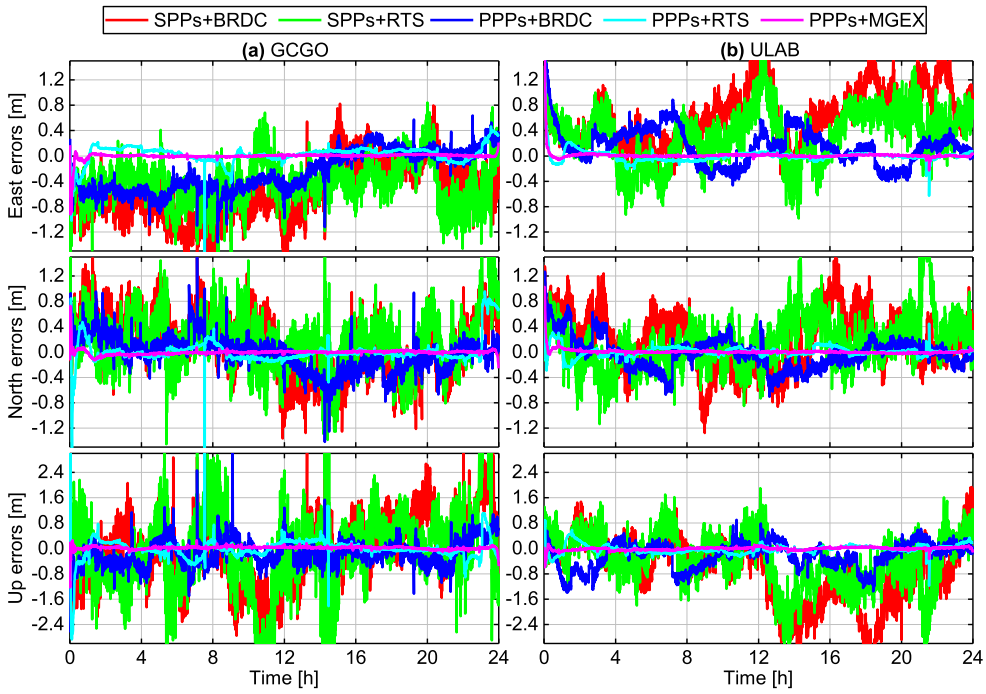


**FIGURE 12.** Daily time series of positioning errors for BDS-2+3 kinematic solutions at stations GCGO and ULAB on DOY 228 of 2021.

### 2) BDS-2+3 POSITIONING ADVANTAGES IN THE ASIA–PACIFIC REGION

As discussed in Section II, the satellite visibility and PDOP of BDS-2+3 is obviously better than that of GPS in the Asia-Pacific region, which give a potential advantage of positioning performance in some harsh observation environments. Therefore, we will investigate the BDS-2+3 positioning advantages in some real harsh environments in

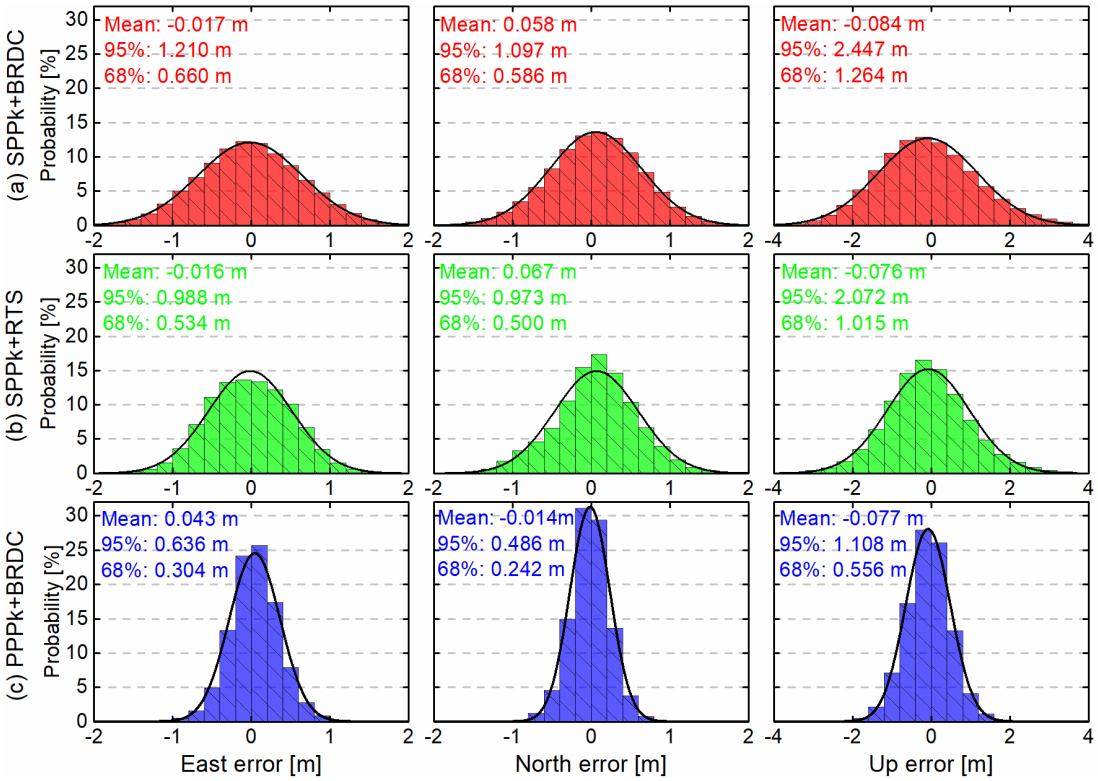


**FIGURE 13.** Probability distributions of positioning errors in the three components on a one-month period for (a) SPPk+BRDC, (b) SPPk+RTS and (c) PPPk+BRDC model.

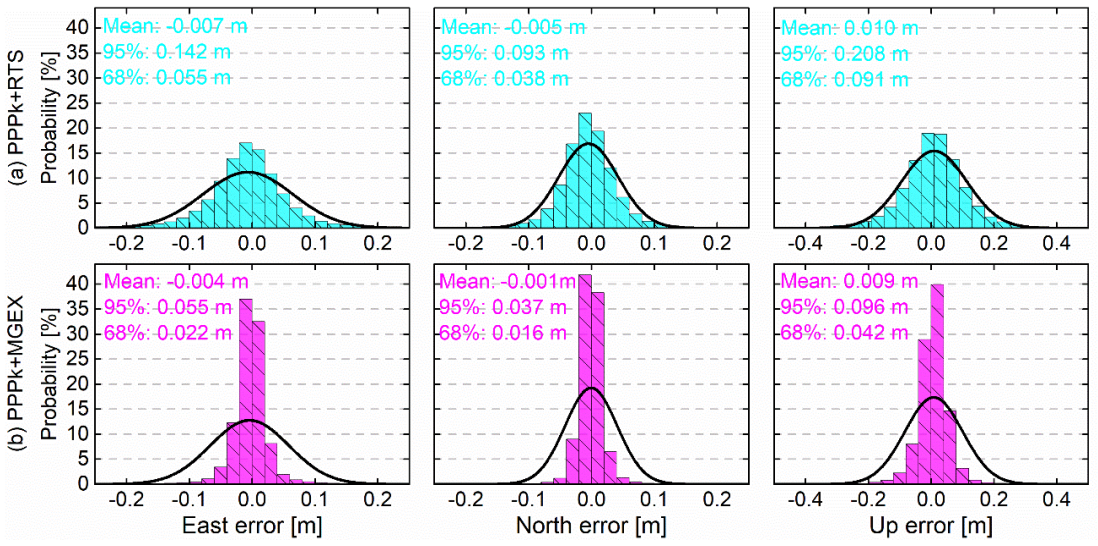


**FIGURE 14.** Probability distributions of positioning errors in the three components on a one-month period for (a) PPPk+RTS and (b) PPPk+MGEX model.

the Asia-Pacific region. For simulating conditions with different obstructed satellite visibility, the cut-off elevations from 7 to 40° and the kinematic positioning mode will be used, so that we can investigate the positioning performance in some real-time dynamic situations. Due to the poor quality of RTS products for BDS-3 and BDS-2 at current stage, only the three kinematic positioning models, i.e., SPPk+BRDC, PPPk+BRDC and PPPk+MGEX are compared for BDS-2+3 and GPS constellations. Five MGEX stations (CUSV, POL2, SGOC, ULAB and WUH2) in the Asia-Pacific region in Fig. 3 are selected to compare the positioning performance of BDS-2+3 and GPS. Figure 15

**TABLE 6.** Dual-frequency sratic positioning accuracies (95%/68%) for BDS-2+3 and GPS AT 7° cut-off elevation (unit:m).

| Mode | East | | North | | Up | | 3D | |
|---|---|---|---|---|---|---|---|---|
| | BDS-2+3 | GPS | BDS-2+3 | GPS | BDS-2+3 | GPS | BDS-2+3 | GPS |
| SPPs+BRDC | 0.743/0.453 | 0.665/0.411 | 0.601/0.365 | 0.612/0.377 | 1.021/0.566 | 1.001/0.551 | 1.281/0.880 | 1.240/0.856 |
| SPPs+RTS | 0.509/0.353 | 0.249/0.185 | 0.404/0.274 | 0.317/0.258 | 0.615/0.338 | 0.573/0.382 | 0.854/0.619 | 0.694/0.535 |
| PPPs+BRDC | 0.239/0.115 | 0.261/0.126 | 0.174/0.096 | 0.216/0.102 | 0.529/0.296 | 0.462/0.251 | 0.575/0.344 | 0.543/0.337 |
| PPPs+RTS | 0.042/0.018 | 0.021/0.011 | 0.026/0.012 | 0.013/0.007 | 0.067/0.034 | 0.027/0.014 | 0.077/0.043 | 0.034/0.021 |
| PPPs+MGEX | 0.014/0.007 | 0.014/0.006 | 0.013/0.007 | 0.011/0.005 | 0.028/0.015 | 0.023/0.012 | 0.031/0.019 | 0.027/0.015 |

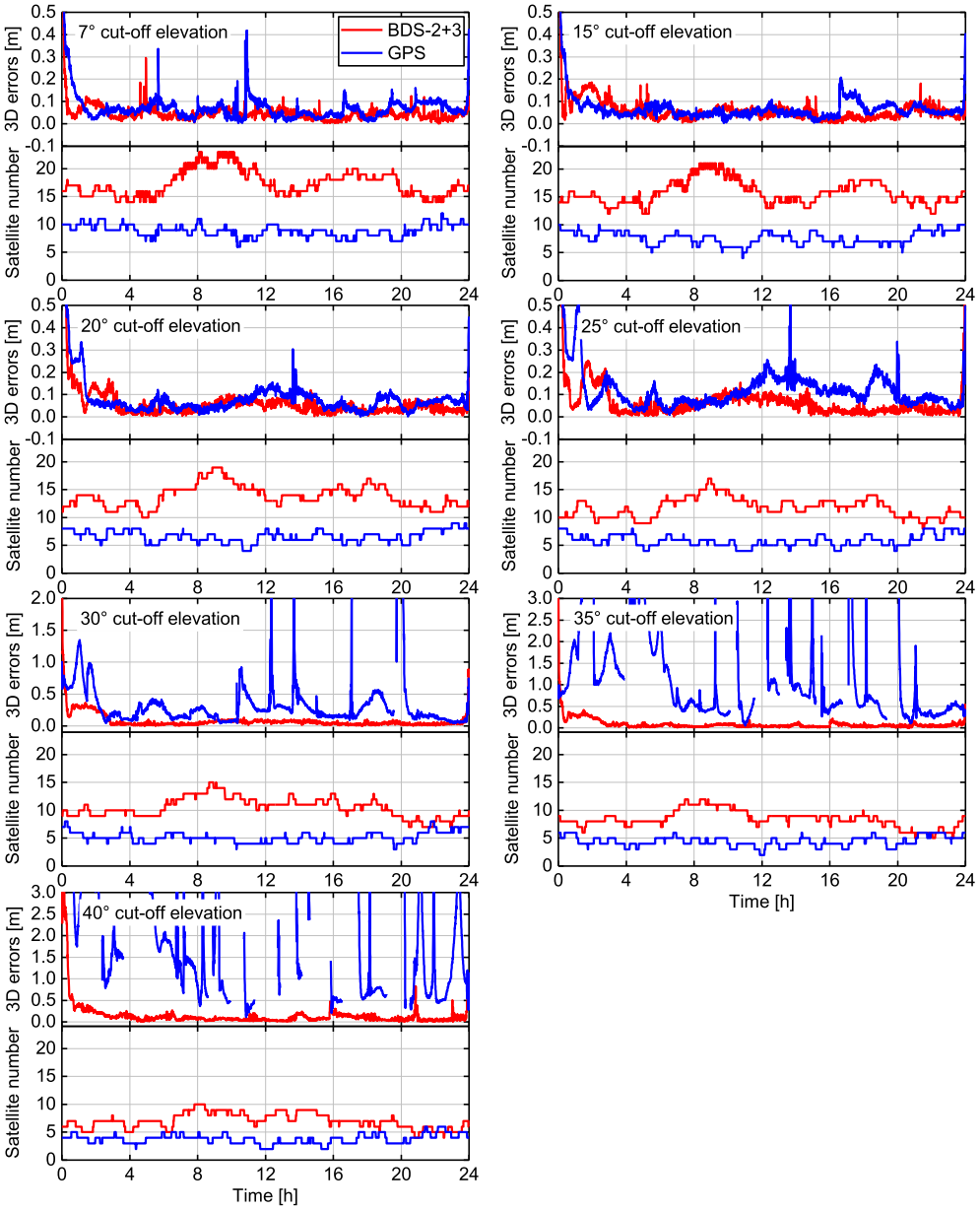


**FIGURE 15.** 3D positioning errors of PPPk+MGEX model and satellite number for BDS-2+3 and GPS constellations at station ULAB with 7°, 15°, 20°, 25°, 30°, 35° and 40° cut-off elevations.

exhibits 3D positioning errors and satellite numbers for station ULAB at 7°, 15°, 20°, 25°, 30°, 35° and 40° cut-off elevations. It can be found that the satellite number of BDS-2+3 is more than that of GPS for various cut-off elevations, which will lead to a better positing performance. With the increase of the cut-off elevation, the positioning accuracies of all the three positioning models are decreased, but the positioning accuracy of BDS-2+3 is better and better than that of GPS,

**TABLE 7.** Dual-frequency kinematic positioning accuracies (95%/68%) for BDS-2+3 and GPS AT 7° cut-off elevation (unit:m).

| Mode | East | | North | | Up | | 3D | |
|---|---|---|---|---|---|---|---|---|
| | BDS-2+3 | GPS | BDS-2+3 | GPS | BDS-2+3 | GPS | BDS-2+3 | GPS |
| SPPk+BRDC | 1.210/0.660 | 1.185/0.598 | 1.097/0.586 | 1.104/0.588 | 2.447/1.264 | 2.312/1.227 | 2.634/1.598 | 2.542/1.525 |
| SPPk+RTS | 0.988/0.534 | 0.613/0.338 | 0.973/0.500 | 0.757/0.432 | 2.072/1.015 | 1.428/0.756 | 2.281/1.314 | 1.564/0.970 |
| PPPk+BRDC | 0.636/0.304 | 0.638/0.319 | 0.486/0.242 | 0.553/0.269 | 1.108/0.556 | 1.158/0.584 | 1.247/0.715 | 1.287/0.756 |
| PPPk+RTS | 0.142/0.055 | 0.063/0.025 | 0.093/0.038 | 0.043/0.018 | 0.208/0.091 | 0.104/0.045 | 0.259/0.123 | 0.123/0.059 |
| PPPk+MGEX | 0.055/0.022 | 0.059/0.020 | 0.037/0.016 | 0.039/0.015 | 0.096/0.042 | 0.097/0.038 | 0.112/0.053 | 0.116/0.050 |

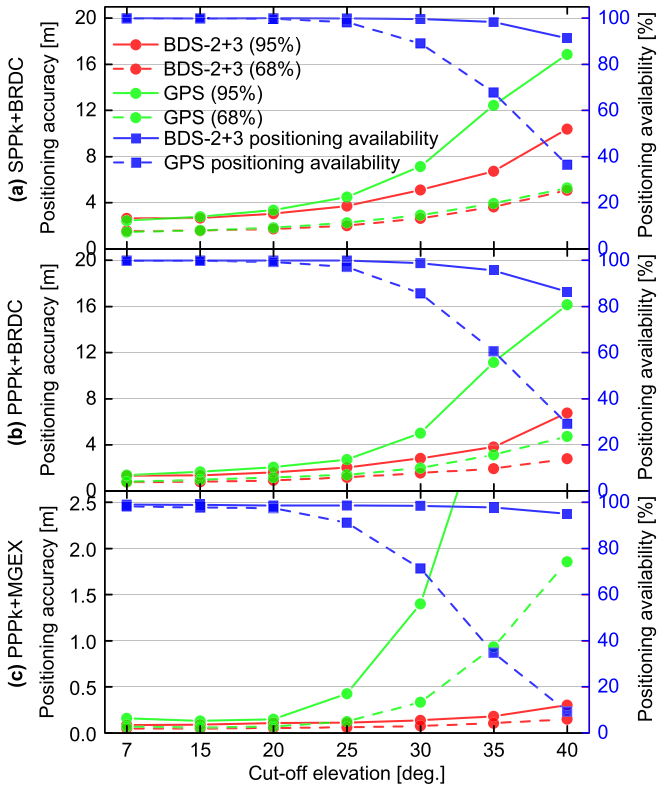


**FIGURE 16.** 3D positioning errors and positioning availability against satellite cut-off elevations for BDS-2+3 and GPS with (a) SPPk+BRDC, (b) PPPk+BRDC and (c) PPPk+MGEX models.

especially at higher cut-off elevations. It shows that BDS-2+3 obtains a better positioning accuracy than GPS in the environments with high cut-off elevations for all three positioning models. These results demonstrate that the BDS-2+3 constellation achieves a better positioning performance in the Asia-Pacific region at higher cut-off elevations as compared to GPS constellation.

The positioning availability of SPPk+BRDC model is defined as that the positioning error is less than 10 m (95%). As for PPPk+BRDC model, the positioning availability is defined as the positioning error less than 5 m. The positioning availability of PPPk+MGEX model is considered to be as less than 0.5 m in the positioning error. The 3D positioning errors and positioning availability against satellite cut-off elevations for BDS-2+3 and GPS with SPPk+BRDC, PPPk+BRDC and PPPk+MGEX models are exhibited in Figure 16. The statistics of positioning error and availability presented in Figure 16 is derived from the positioning solutions of five stations in the Asia-Pacific region. It can be found that the 3D positioning accuracy of BDS-2+3 is comparable to that of GPS with lower than 20° cut-off elevations. As expected, the positioning accuracy of BDS-2+3 is higher and higher than that of GPS with the cut-off elevation increasing. On the other hand, the positioning availability of GPS is dropped dramatically with higher than 25° cut-off elevations for all three positioning models. Nevertheless, the positioning availability of BDS-2+3 can still maintain a high level even at 35° or 40° cut-off elevation. It can be concluded that BDS-2+3 combined system has the comparable performance of absolute positioning using BRDC or final MGEX product in a global scale, and even better one in the Asia-Pacific region with higher cut-off elevations as compared to GPS system.

## VI. SUMMARY AND CONCLUSION

After the completion of global BDS-3 constellation, the satellite visibility and positioning geometry of BDS-2+3 are almost the same as GPS and even far superior to GPS in

Asia-Pacific region. In this contribution, the performance of dual-frequency absolute positioning using the fully serviceable BDS-2+3 constellation was comprehensively evaluated and compared to the GPS positioning performance. The various satellite orbit and clock i.e., broadcast ephemerides, RTS and final MGEX products are used to access the positioning performance of SPP and PPP in both static and kinematic modes. The accuracy of broadcast orbit and clock of BDS-3 has been obviously improved compared to BDS-2 and is comparable to that of GPS. In addition, the accuracy of RTS product of BDS-2 and BDS-3 is worse than that of GPS at the current stage.

As for SPP using broadcast ephemerides, BDS-2+3 can achieve the positioning accuracy of 0.743/0.601/1.021 m (95%) and 0.453/0.365/0.566 m (68%) in east/north/up components in static mode as well as 1.210/1.097/2.447 m (95%) and 0.660/0.586/1.264 m (68%) in kinematic mode, which are equivalent to those of GPS. The positioning accuracy of SPP using RTS product of BDS-2+3 is obviously worse than that of GPS due to the poor accuracy of RTS products of BDS-2 and BDS-3. The positioning accuracy of PPP using broadcast ephemerides of BDS-2+3 is comparable to that of GPS, and can reach 0.239/0.174/0.529 m (95%) and 0.115/0.096/0.296 m (68%) in static mode and 0.636/0.486/1.108 m (95%) and 0.304/0.242/0.556 m (68%) in kinematic mode. However, the positioning accuracy of PPP using RTS product of BDS-2+3 is obviously worse than that of GPS, because of BDS RTS products with poor accuracy. As for PPP using final MGEX product, BDS-2+3 constellation attains the positioning accuracy of 0.014/0.013/0.028 m (95%) and 0.007/0.007/0.015 m (68%) in static mode and 0.055/0.037/0.096 m (95%) and 0.022/0.016/0.042 m (68%) in kinematic mode, which are competitive to GPS positioning accuracy.

The satellite visibility and PDOP of BDS-2+3 are obviously better than that of GPS in Asia-Pacific region, which give a potential advantage of positioning performance in some harsh observation environments. The BDS-2+3 constellation achieves a better positioning performance in Asia-Pacific region at higher cut-off elevations as compared to GPS constellation for both SPP and PPP models using RTS or final MGEX product.

With the increasing of tracking stations and more focus on BDS-3, the positioning accuracy of BDS could be further improved in the future with more accurate BDS precise products of orbit, clock and PCO/PCV corrections.

## REFERENCES


[1] Y. Yang, J. Li, J. Xu, J. Tang, H. Guo, and H. He, "Contribution of the compass satellite navigation system to global PNT users," *Chin. Sci. Bull.*, vol. 56, no. 26, pp. 2813–2819, Aug. 2011, doi: 10.1007/s11434-011-4627-4.

[2] X. Zhang, M. Wu, W. Liu, X. Li, S. Yu, C. Lu, and J. Wickert, "Initial assessment of the COMPASS/BeiDou-3: New-generation navigation signals," *J. Geodesy*, vol. 91, no. 10, pp. 1225–1240, 2017, doi: 10.1007/s00190-017-1020-3.

[3] Y. Yang, Y. Xu, J. Li, and C. Yang, "Progress and performance evaluation of BeiDou global navigation satellite system: Data analysis based on BDS-3 demonstration system," *Sci. China Earth Sci.*, vol. 61, no. 5, pp. 614–624, May 2018, doi: 10.1007/s11430-017-9186-9.

[4] X. Xie, T. Geng, Q. Zhao, J. Liu, and B. Wang, "Performance of BDS-3: Measurement quality analysis, precise orbit and clock determination," *Sensors*, vol. 17, no. 6, p. 1233, May 2017, doi: 10.3390/s17061233.

[5] C. Hu, Q. Wang, Z. Wang, and A. H. Moraleda, "New-generation BeiDou (BDS-3) experimental satellite precise orbit determination with an improved cycle-slip detection and repair algorithm," *Sensors*, vol. 18, no. 5, p. 1402, May 2018, doi: 10.3390/s18051402.

[6] X. Ren, Y. Yang, J. Zhu, and T. Xu, "Orbit determination of the next-generation BeiDou satellites with intersatellite link measurements and a priori orbit constraints," *Adv. Space Res.*, vol. 60, no. 10, pp. 2155–2165, Nov. 2017, doi: 10.1016/j.asr.2017.08.024.

[7] W. Liu, M. Wu, X. Zhang, W. Wang, W. Ke, and Z. Zhu, "Single-epoch RTK performance assessment of tightly combined BDS-2 and newly complete BDS-3," *Satell. Navigat.*, vol. 2, no. 1, pp. 1–17, Apr. 2021, doi: 10.1186/s43020-021-00038-y.

[8] Y. Zhang, N. Kubo, J. Chen, J. Wang, and H. Wang, "Initial positioning assessment of BDS new satellites and new signals," *Remote Sens.*, vol. 11, no. 11, p. 1320, Jun. 2019, doi: 10.3390/rs11111320.

[9] M. Wu, W. Liu, W. Wang, and X. Zhang, "Differential inter-system biases estimation and initial assessment of instantaneous tightly combined RTK with BDS-3, GPS, and Galileo," *Remote Sens.*, vol. 11, no. 12, p. 1430, Jun. 2019, doi: 10.3390/rs11121430.

[10] G. Chen, B. Li, Z. Zhang, and T. Liu, "Integer ambiguity resolution and precise positioning for tight integration of BDS-3, GPS, GALILEO, and QZSS overlapping frequencies signals," *GPS Solutions*, vol. 26, no. 1, p. 26, Jan. 2022, doi: 10.1007/s10291-021-01203-1.

[11] China Satellite Navigation Office. *BeiDou Navigation Satellite System Open Service Performance Standard (Version 2.0)*. Dec. 2018. [Online]. Available: http://www.beidou.gov.cn/xt/gfxz/201812/P020181227529449178798.pdf

[12] Y. Zhang, N. Kubo, J. Chen, F.-Y. Chu, A. Wang, and J. Wang, "Apparent clock and TGD biases between BDS-2 and BDS-3," *GPS Solutions*, vol. 24, no. 1, p. 27, Dec. 2019, doi: 10.1007/s10291-019-0933-0.

[13] Y. Zhang, H. Wang, J. Chen, A. Wang, L. Meng, and E. Wang, "Calibration and impact of BeiDou satellite-dependent timing group delay bias," *Remote Sens.*, vol. 12, no. 1, p. 192, Jan. 2020, doi: 10.3390/rs12010192.

[14] P. Dai, Y. Ge, W. Qin, and X. Yang, "BDS-3 time group delay and its effect on standard point positioning," *Remote Sens.*, vol. 11, no. 15, p. 1819, Aug. 2019, doi: 10.3390/rs11151819.

[15] G. Jiao, S. Song, Y. Liu, K. Su, N. Cheng, and S. Wang, "Analysis and assessment of BDS-2 and BDS-3 broadcast ephemeris: Accuracy, the datum of broadcast clocks and its impact on single point positioning," *Remote Sens.*, vol. 12, no. 13, p. 2081, Jun. 2020, doi: 10.3390/rs12132081.

[16] O. Montenbruck and R. C. Rizos, "Weber getting a grip on multi-GNSS–The international GNSS service MGEX campaign," *GPS World*, vol. 24, no. 7, pp. 44–49. Jul. 2013.

[17] G. Jiao, S. Song, and W. Jiao, "Improving BDS-2 and BDS-3 joint precise point positioning with time delay bias estimation," *Meas. Sci. Technol.*, vol. 31, no. 2, Feb. 2020, Art. no. 025001, doi: 10.1088/1361-6501/ab41cf.

[18] W. Zhao, H. Chen, Y. Gao, W. Jiang, and X. Liu, "Evaluation of inter-system bias between BDS-2 and BDS-3 satellites and its impact on precise point positioning," *Remote Sens.*, vol. 12, no. 14, p. 2185, Jul. 2020, doi: 10.3390/rs12142185.

[19] S. Zhu, D. Yue, L. He, J. Chen, and Z. Liu, "Modeling and performance assessment of BDS-2/BDS-3 triple-frequency ionosphere-free and uncombined precise point positioning," *Measurement*, vol. 180, Aug. 2021, Art. no. 109564, doi: 10.1016/j.measurement.2021.109564.

[20] X. Cao, F. Shen, S. Zhang, and J. Li, "Time delay bias between the second and third generation of BeiDou navigation satellite system and its effect on precise point positioning," *Measurement*, vol. 168, Jan. 2021, Art. no. 108346, doi: 10.1016/j.measurement.2020.108346.

[21] T. Hadas, K. Kazmierski, and K. Sośnica, "Performance of galileo-only dual-frequency absolute positioning using the fully serviceable Galileo constellation," *GPS Solutions*, vol. 23, no. 4, p. 108, Aug. 2019, doi: 10.1007/s10291-019-0900-9.

[22] L. Carlin, A. Hauschild, and O. Montenbruck, "Precise point positioning with GPS and Galileo broadcast ephemerides," *GPS Solutions*, vol. 25, no. 2, p. 77, Mar. 2021, doi: 10.1007/s10291-021-01111-4.

[23] L. Qu, M. Du, J. Wang, Y. Gao, Q. Zhao, Q. Zhang, and X. Guo, "Precise point positioning ambiguity resolution by integrating BDS-3e into BDS-2 and GPS," *GPS Solutions*, vol. 23, no. 3, p. 63, Jul. 2019, doi: 10.1007/s10291-019-0854-y.
[24] J. Shi, C. Ouyang, Y. Huang, and W. Peng, "Assessment of BDS-3 global positioning service: Ephemeris, SPP, PPP, RTK, and new signal," *GPS Solutions*, vol. 24, no. 3, p. 81, Jun. 2020, doi: 10.1007/s10291-020-00995-y.
[25] E. Schönemann, M. Becker, and T. Springer, "A new approach for GNSS analysis in a multi-GNSS and multi-signal environment," *J. Geodetic Sci.*, vol. 1, no. 3, pp. 204–214, Jan. 2011, doi: 10.2478/v10156-010-0023-2.
[26] Y. Zhang, N. Kubo, J. Chen, F.-Y. Chu, A. Wang, and J. Wang, "Apparent clock and TGD biases between BDS-2 and BDS-3," *GPS Solutions*, vol. 24, no. 1, p. 27, Dec. 2019, doi: 10.1007/s10291-019-0933-0.
[27] O. Montenbruck, P. Steigenberger, and A. Hauschild, "Broadcast versus precise ephemerides: A multi-GNSS perspective," *GPS Solutions*, vol. 19, no. 2, pp. 321–333, Jun. 2014, doi: 10.1007/s10291-014-0390-8.
[28] Y. Yang, W. Gao, S. Guo, Y. Mao, and Y. Yang, "Introduction to BeiDou-3 navigation satellite system," *Navigation*, vol. 66, no. 1, pp. 7–18, 2019, doi: 10.1002/navi.291.
[29] S. Gu, F. Mao, X. Gong, Y. Lou, X. Xu, and Y. Zhou, "Evaluation of BDS-2 and BDS-3 satellite atomic clock products and their effects on positioning," *Remote Sens.*, vol. 13, no. 24, p. 5041, Dec. 2021, doi: 10.3390/rs13245041.
[30] F. Guo, X. Li, X. Zhang, and J. Wang, "Assessment of precise orbit and clock products for Galileo, BeiDou, and QZSS from IGS multi-GNSS experiment (MGEX)," *GPS Solutions*, vol. 21, no. 1, pp. 279–290, Jan. 2017, doi: 10.1007/s10291-016-0523-3.
[31] O. Montenbruck, P. Steigenberger, and A. Hauschild, "Multi-GNSS signal-in-space range error assessment—Methodology and results," *Adv. Space Res.*, vol. 61, no. 12, pp. 3020–3038, Jun. 2018, doi: 10.1016/j.asr.2018.03.041.

**SHENGNAN LIU** received the B.S. and M.S. degrees in surveying and mapping engineering from Hohai University, Nanjing, China, in 2009 and 2012, respectively, where she is currently pursuing the Ph.D. degree in geodesy with the School of Earth Sciences and Engineering. Her research interests include data processing for global navigation satellite systems (GNSS), precise point positioning, and GNSS remote sensing.

**SHAOLIN ZHU** received the B.S. degree in surveying and mapping engineering from East China Jiaotong University, Nanchang, China, in 2015, and the M.S. and Ph.D. degrees in geodesy from Hohai University, Nanjing, China, in 2018 and 2022, respectively. His research interests include global navigation satellite systems (GNSS), precise point positioning, and real-time kinematic (RTK) positioning and related applications.

**JIAN ZHANG** received the B.S. degree in surveying and mapping engineering from Hohai University, Nanjing, China, in 2009. He is currently working with the Powerchina Qinghai Electric Power Design Institute Company Ltd., where he engaged in power measurement for 13 years, as a Senior Engineer and the Chief Engineer. His research interests include global navigation satellite systems (GNSS), precise point positioning, and related applications.